Di-, Tri-, and Tetrametallic Double-Stranded Helical Complexes Derived from Alkylthio-Substituted Septipyridines: Synthesis, Structure, and Redox Properties[1]

Kevin T. Potts,*,† Majid Keshavarz-K,† Fook S. Tham,† Kimberly A. Gheysen Raiford,† Claudia Arana,‡ and Héctor D. Abruña*,‡

Departments of Chemistry, Rensselaer Polytechnic Institute, Troy, New York 12181, and Cornell University, Ithaca, New York 14853

Received May 14, 1993®

4′,4‴′-Bis(methylthio)-4″,4‴′-bis(*n*-propylthio)septipyridine (**1**), a new heptadentate ligand, reacted with Co(II) acetate at ambient temperature yielding a bimetallic complex of composition $[LCo^{II}]_2[PF_6]_4$. The complex crystallized in the triclinic space group *P*1 (No. 2) with unit cell dimensions $a = 15.561(4)$ Å, $b = 16.879(4)$ Å, $c = 20.632(5)$ Å, $\alpha = 80.02(2)°$, $\beta = 81.88(2)°$, and $\gamma = 74.92(2)°$, with $V = 5127(2)$ Å^3 and $Z = 2$. The X-ray data showed that the two ligand strands were intertwined about each other and around the two Co(II) cations in a double-helical fashion. Each ligand strand acted as two discrete terpyridine units, and in one strand, pyridine ring one was uncoordinated, while, in the other strand, ring four was uncoordinated. Both Co(II) ions have distorted octahedral geometry (N_6, N_6), and the Co–Co distance was 4.606 Å. The cyclic voltammogram of the complex showed a metal-based, two-electron oxidation as well as three ligand based reduction waves. Bi-, tri-, and tetrametallic double-helical complexes resulted from reaction of the ligand **1** and copper ions of both oxidation states under different reaction conditions. Their compositions were established by a combination of combustion analytical data, FAB mass spectral data, and electrochemical data. Redox-induced transformations among this group of copper helicates were established spectroelectrochemically. An intramolecular diastereotopic effect in the ^{1}H NMR spectrum of the diamagnetic, tetrametallic complex showed its chiral nature and its stability in solution. An absorption at 1420 nm in the near infrared spectrum of the mixed-valence, trimetallic complex is attributed to an intervalence electron-transfer transition.

Introduction

Self-assembling processes allow the construction of functional, supramolecular entities from simple, prefabricated molecular components,[2] and metal ion-induced self-assembly has been used as a synthetic technique for the preparation of mono-,[3] double-,[4] and triple[5] -stranded helical complexes from several polydentate ligands. Metal–metal interactions[6,7] and intramolecular electron transfer are areas of continuing interest. We have been conducting a systematic study of these areas using tetrapyridylpyrazine complexes,[8] and also multimetallic, double-stranded helical complexes derived from oligopyridines and transition metals.[4g,9] The self-assembly process spontaneously positions the metals in close proximity to one another, resulting in an excellent series of models of well-defined structure. Cu(I) complexes which may adopt a variety of coordination geometries are of particular interest. In our work to date, even numbered alkylthio-substituted oligopyridines resulted in complexes containing Cu(I) centers with distorted tetrahedral geometry {analogous to that present in the bis(bipyridine)–Cu(I) $[L_2Cu^I]^{1+}$ complex[10] }, consistent with each ligand strand acting as a number of discrete bipyridine subunits; i.e., quaterpyridines, sexipyridines, and octipyridines formed bimetallic $[L_2Cu(I)_2]^{2+}$, trimetallic $[L_2Cu^I_3]^{3+}$, and tetrametallic $[L_2Cu^I_4]^{4+}$ complexes[9], respectively. In contrast, complexes derived from odd-numbered oligopyridines present a different situation. 6′,6″-Diphenyl(alkylthio)terpyridines[4g,11] and the alkylthio-substituted quinquepyridines[9] formed bimetallic $[L_2Cu^I_2]^{2+}$ and trimetallic $[L_2Cu^I_3]^{3+}$ double-helical complexes,

† Rensselaer Polytechnic Institute.
‡ Cornell University.
* Abstract published in *Advance ACS Abstracts,* October 1, 1993.

(1) (a) Part 5 in the series Metal Ion-Induced Self-Assembly of Functionalized 2,6-Oligopyridines. (b) Abstracted in part from the Ph.D. dissertations of M.K. (1993), Rensselaer Polytechnic Institute, and C.A. (1993), Cornell University.
(2) Lehn, J.-M. *Angew. Chem., Int. Ed. Engl.* **1990**, *29*, 1304. Pfiel, A.; Lehn, J.-M. *J. Chem. Soc., Chem. Commun.* **1992**, 8839. Schneider, H.-J.; Dürr, H. *Frontiers in Supra-molecular Organic Chemistry and Photochemistry;* VCH: Weinheim, Germany, 1991. Stoddart, J. F. *Annual Reports, Section B: Organic Chemistry;* Royal Society of Chemistry: London, 1988, 385. Whitesides, G. M.; Mathias, J. P.; Seto, C. T. *Science* **1991**, *254*, 1312. Vögtle, F. *Supramolecular Chemistry;* Wiley: Chichester, U.K., 1991.
(3) (a) Gheysen, K. A.; Potts, K. T.; Hurrell, H. C.; Abruña, H. D. *Inorg. Chem.* **1990**, *29*, 1589. (b) Constable, E. C.; Drew, M. G. B.; Forsyth, G.; Ward, M. D. *J. Chem. Soc., Chem. Commun.* **1988**, 1450. Constable, E. C.; Chotalia, R.; Tocher, D. A. *J. Chem. Soc., Chem. Commun.* **1992**, 771.
(4) (a) Lehn, J.-M.; Sauvage, J.-P.; Simon, J.; Ziessel, R.; Piccinni-Leopardi, C.; Germain, G.; Declerq, J.-P.; Van Meerssche, M. *Nouv. J. Chem.* **1983**, *7*, 413. (b) Lehn, J.-M.; Rigault, A.; Siegel, J.; Harrowfield, J.; Chevrier, B.; Moras, D. *Proc. Natl. Acad. Sci. U.S.A.* **1987**, *84*, 2565. (c) Lehn, J.-M.; Rigault, A. *Angew. Chem., Int. Ed. Engl.* **1988**, *27*, 1095. (d) Constable, E. C.; Hannon, M. J.; Martin, A.; Raithby, P. R.; Tocher, D. A. *Polyhedron* **1992**, *11*, 2967 and references listed therein. (e) Constable, E. C. *Tetrahedron* **1992**, *46*, 10014. (f) Potts, K. T. *Bull. Soc. Chim. Belg.* **1990**, *90*, 741. (g) Potts, K. T.; Keshavarz-K, M.; Tham, F. S.; Arana, C.; Abruña, H. D. *Inorg. Chem.* **1993**, *32*, 4422, 4439.
(5) Bernardinelli, G.; Piguet, C.; Williams, A. F. *Angew Chem., Int. Ed. Engl.* **1992**, *31*, 1622. Ruttimann, S.; Piguet, C.; Bernardinelli, G.; Bocquet, B.; Williams, A. F. *J. Am. Chem. Soc.* **1992**, *114*, 114.
(6) Gagne, R. R.; Spiro, C. L. *J. Am. Chem. Soc.* **1980**, *102*, 1443. Powers, J. M.; Meyer, T. J. *J. Am. Chem. Soc.* **1980**, *102*, 1389. Campagna, S.; Denti, G.; Serroni, S.; Ciano, M.; Balzani, V. *Inorg. Chem.* **1991**, *30*, 3728. Balzani, V.; Scandola, F. *Supra-molecular Photochemsitry;* Horwood: Chichester, U.K., 1991.
(7) Creutz, C.; Taube, H. *J. Am. Chem. Soc.* **1969**, *91*, 3988. Stein, C. A.; Taube, H. *J. Am. Chem. Soc.* **1981**, *103*, 693. Richardson, D. E.; Taube, H. *J. Am. Chem. Soc.* **1983**, *105*, 40. Meyer, T. J. *Acc. Chem. Res.* **1978**, *11*, 94. Waitellier, S.; Launay, J. P.; Spangler, C. W. *Inorg. Chem.* **1989**, *28*, 758.
(8) Arana, C.; Abruña, H. D. *Inorg. Chem.* **1993**, *32*, 194. For similar complexes see also: Launay, J.-P.; Sauvage, J.-P.; Sour, A. *J. Chem. Soc., Chem. Commun.* **1993**, 434.
(9) Potts, K. T.; Keshavarz-K, M.; Tham, F. S.; Arana, C.; Abruña, H. D. *Inorg. Chem.* **1993**, *32*, 4450.
(10) Munakata, M.; Kitagawa, S.; Asahara, A.; Masuda, H. *Bull Chem. Soc. Jpn.* **1987**, *60*, 1927.
(11) Crumbliss, A. L.; Poulos, A. T. *Inorg. Chem.* **1975**, *14*, 1529. Manakata, M.; Nishibayashi, S.; Sakamoto, H. *J. Chem. Soc., Chem. Commun.* **1980**, 219. Pflaum, R. T.; Brandt, W. W. *J. Am. Chem. Soc.* **1955**, *77*, 2019. Chandra, M.; O'Driscoll, K. F.; Rempel, G. L. *Prep. Can. Symp. Catal.* **1979**, *6*, 44. *J. Mol. Catal.* **1980**, *8*, 339.

0020-1669/93/1332-5477$04.00/0

respectively, which had distorted tetrahedral and linear coordination geometries. ^{1}H NMR data showed them to have a symmetrical geometry (D_2 symmetry) in solution. Differences in the formal potentials ($\Delta E^{\circ\prime}$ = 860 mV for the bimetallic terpyridine complex and 530, 540 mV for the trimetallic quinquepyridine complex) between the Cu centers indicated the presence of significant metal–metal interactions. The quinquepyridine ligand also formed a mixed-valence complex $[L_2\text{-}Cu^{II}/Cu^{I}]^{3+}$, whose copper ions had distorted octahedral and distorted tetrahedral geometries, respectively. An intervalence electron transfer (IT) transition centered at 1414 nm was clear evidence[7] for electron delocalization and metal–metal coupling between the two copper centers in this complex.

We describe here the coordination behavior of a new, odd-numbered oligopyridine, 4′,4‴″-bis(methylthio)-4″,4‴″-bis(*n*-propylthio)septipyridine (at-septipy) (**1**), a heptadentate ligand that is not preorganized by steric or other factors which would favor its segmentation into discrete subunits. Thus, any encoded information is recognized by the metal ion used in the self-assembly process and, conceptually, this ligand may behave as [(bipy)$_3$-(pyridine)], [(bipy)$_2$(terpy)], [(terpy)$_2$(pyridine)], [(quaterpy)-(terpy)], and [(qnpy)(bipy)], among others. The septipyridine **1** is one of a series of oligopyridines described[12] recently which were designed to take advantage of substituents in the 4-position of selected pyridine rings. Solubility enhancement in organic solvents, enabling the self-assembly to be carried out under mild reaction conditions, organic functional group interconversions,[13] and utilization in NMR studies, as described below, are important attributes of these alkylthio-substituted oligopyridines.

Experimental Section

Electrochemical and spectroscopic measurements were performed in acetonitrile (Burdick and Jackson distilled in glass, dried over 4-Å molecular sieves), and the supporting electrolyte was tetra-*n*-butylammonium perchlorate (TBAP) (G.F.S. Chemicals), which was recrystallized three times from EtOAc and dried under vacuum for 72 h. Supporting electrolyte concentrations were 0.1 M unless otherwise indicated. All electrochemical experiments were performed using a platinum disk electrode (A = 0.08 cm^2), which was polished prior to use with 1-μm diamond paste (Buehler) and rinsed thoroughly with water and acetone. A sodium saturated calomel electrode (SSCE) was used as reference without regard for the liquid junction potential. A coiled platinum wire formed the counter electrode, and electrochemical cells were of conventional design. Solutions for electrochemistry were typically millimolar in the redox species and were deoxygenated by purging with prepurified nitrogen for at least 10 min. Unless otherwise stated, the sweep rate in cyclic voltammetric experiments was 100 mV/s.

The electrochemical instrumentation utilized was either a Pine Instrument Co. Model RDE3 Electrochemical Analyzer or a PAR Model 173 potentiostat in conjunction with a PAR Model 179 universal programmer. Data were recorded on a Soltec Model VP-6423S recorder. Ultraviolet–visible spectra were obtained using a Hewlett Packard 8451A diode array spectrophotometer in conventional 1-cm quartz cells. Spectroelectrochemical experiments were carried out in a three-compartment Pyrex cell with the central compartment placed in the light path of the spectrophotometer. The working electrode was a 0.5-cm^2 piece of Pt gauze (52 mesh, Aldrich), and electrical contact was made through a Pt wire spot welded to the Pt gauze. The counter and reference electrodes used for these experiments were as described above.

Mass spectral data were obtained on a VG ZAB-SE spectrometer with 3-nitrobenzyl alcohol as matrix, at the University of Illinois.[14] ^{1}H NMR spectra were determined on a Varian 500 MHz NMR spectrometer using TMS as internal standard. FT-IR measurements were made on a Perkin-Elmer FT-IR near-IR spectrophotometer, and combustion analyses were performed by Quantitative Technologies, Inc., Whitehouse, NJ.

Preparation of the [(at-septipy)Co$^{II}_2$][PF$_6$]$_4$ Complex (2). The ligand (at-septipy)[12] (**1**) (100 mg, 1.28 × 10^{-4} mol) was added to a solution of Co(OAc)$_2$·4H$_2$O (64 mg, 2.55 × 10^{-4} mol) in CH$_3$OH (20 mL). The orange solution was stirred for 90 min at 25 °C and was then treated with a saturated methanolic solution of NH_4PF_6 (200 mg). The resultant green salt was collected (166 mg), washed with CH$_3$OH, and recrystallized from CH_3NO_2/Et_2O forming green prisms: 141 mg; yield 97%; mp > 300 °C; MS (FAB, 3-nitrobenzyl alcohol) m/z 2116.7 (4) [M$^+$ – PF$_6$], 1971.9 (2) [M$^+$ – 2PF$_6$], 1827.1 (2) [M$^+$ – 3PF$_6$]. *Anal.* Calcd for $C_{86}H_{78}Co_2F_{24}N_{14}P_4S_8\cdot H_2O$: C, 45.30; H, 3.54; N, 8.60. Found: C, 45.09; H, 3.32; N, 8.52.

Preparation of the [(at-septipy)Cu$^{II}_2$][PF$_6$]$_4$ Complex (3). The ligand **1** (100 mg, 1.28 × 10^{-4} mol) was added to a solution of copper mandelate (93 mg, 2.55 × 10^{-4} mol) (or copper acetate) in CH$_3$OH (15 mL), and after stirring of the resulting green solution for 60 min at 25 °C, a saturated methanolic solution of NH_4PF_6 (150 mg) was added. The separated green salt was collected, washed with CH$_3$OH (120 mg), and recrystallized from CH_3NO_2/Et_2O forming green prisms: 106 mg; yield 73%; mp > 300 °C; MS (FAB, 3-nitrobenzyl alcohol) m/z 2126.7 (8) [M$^+$ – PF$_6$], 1980.4 (100) [M$^+$ – 2PF$_6$], 1691.2 (26) [M$^+$ – 4PF$_6$]. *Anal.* Calcd for $C_{86}H_{78}Cu_2F_{24}N_{14}P_4S_8\cdot 2H_2O$: C, 44.77; H, 3.40; N, 8.50. Found: C, 44.85; H, 3.37; N, 8.38.

Preparation of the [(at-septipy)$_2$Cu^{II}/Cu$^{I}_2$][PF$_6$]$_4$ Mixed-Valence Complex (4). The ligand **1** (200 mg, 2.55 × 10^{-4} mol) was added to a colorless solution of [(CH$_3$CN)$_4$Cu(I)][PF$_6$] (190 mg, 5.1 × 10^{-4} mol) in CH$_3$CN (20 mL). The immediate formation of a brown solution marked complex formation. After stirring of the reaction solution at 25 °C for 2 h, a black complex was precipitated by the addition of Et$_2$O, collected, washed with CH$_3$CN:Et$_2$O (1:1), and air dried (311 mg). It crystallized from CH_3NO_2:Et$_2$O as black prisms: 265 mg; yield 89%; MS (FAB, 3-nitrobenzyl alcohol) m/z 2190.3 (11) [M$^+$ – PF$_6$], 2045.3 (7) [M$^+$ – 2PF$_6$], 1899.1 (12) [M$^+$ – 3PF$_6$]. *Anal.* Calcd for $C_{86}H_{78}Cu_3F_{24}N_{14}P_4S_8\cdot 2H_2O$: C, 43.57; H, 3.43; N, 8.27. Found: C, 43.44; H, 3.27; N, 8.21.

Preparation of the [(at-septipy)$_2$Cu$^{I}_4$][PF$_6$]$_4$ Complex (5). The ligand **1** (200 mg, 2.55 × 10^{-4} mol) was added to a colorless solution of [(CH$_3$-CN)$_4$Cu(I)][PF$_6$] (190 mg, 5.1 × 10^{-4} mol) in oxygen-free CH$_3$OH (20 mL), the reaction system being under a dry N$_2$ atmosphere. The initial, colorless solution immediately changed to a dark-brown color, indicative of complex formation. After stirring of this brown solution for 3 h at 25 °C, the brown product that separated was collected under a nitrogen atmosphere and immediately dried in a vacuum desiccator: 293 mg; yield 96%; MS (FAB, 3-nitrobenzyl alcohol) m/z 2189.5 (2) [M$^+$ – Cu – PF$_6$], 2045.8 (6) [M$^+$ – Cu – 2PF$_6$], 1900 (2) [M – Cu – 3PF$_6$]; ^{1}H NMR (500 MHz, CD_3NO_2) δ 8.19 (t, J = 7.8 Hz, 2H), 7.91 (dt, J = 7.8, J = 1.2Hz, 4H), 7.82 (d, J = 1.2 Hz, 4H), 7.76 (d, J = 8.1 Hz, 4H), 7.67 (d, J = 7.8 Hz, 4H), 7.62 (d, J = 4.4 Hz, 4H), 7.46 (d, J = 1.2 Hz, 4H), 7.40 (d, J = 1.2 Hz, 4H), 7.31 (m, 4H), 7.24 (d, J = 1.2 Hz, 4H), 3.20 (m, 8H), 2.74 (s, 12H), 2.06 (H$_2$O), 1.86 (m, 8H), 1.18 (t, 12H). *Anal.* Calcd for $C_{86}H_{78}Cu_4F_{24}N_{14}P_4S_8\cdot H_2O$: C, 42.75; H, 3.33; N, 8.12. Found: C, 42.67; H, 3.19; N, 8.07.

X-ray Structural Determination. Crystal Data for 2. Crystals of **2**, $C_{86}H_{78}Co_2N_{14}S_8(PF_6)_4\cdot 1.75CH_3NO_2\cdot 0.65CH_3OH$, were grown from nitromethane with the slow diffusion of diethyl ether. A green prism (0.24 × 0.48 × 0.64 mm) was chosen and mounted (cold room, 2 °C) by dipping the crystal in epoxy resin and attaching it onto a glass fiber before the epoxy hardened: M = 2389.18, triclinic $P\bar{1}$ (No. 2), unit cell dimensions a = 15.561(4) Å, b = 16.879(4) Å, c = 20.632(5) Å, α = 80.02(2)°, β = 81.88(2)°, and γ = 74.92(2)° based on 25 centered reflections (21.50° ≤ 2θ ≤ 25.34°), with V = 5127 (2) Å^3, and Z = 2. Data collection was carried out at 25 °C using a Siemens R3m diffractometer with Mo Kα radiation (graphite monochromator; λ = 0.710 69 Å) in a Wyckoff scan mode (ω range = 1.50° + [2θ(K$_{\alpha 1}$) – 2θ(K$_{\alpha 2}$)]; 2θ range = 3–48°). The reflections were measured with a variable scan speed (5.00–29.30°/min) and an ω scan range of 1.50°. Four standard reflections were measured for every 60 reflections; 16 942 reflections were collected of which 10 293 reflections were uniquely observed ($F > 4.0\sigma(F)$). Lorentz, polarization, and semi-empirical absorption corrections were applied [μ(Mo) = 0.65 mm^{-1}; maximum and minimum transmission factors are 0.667 and 0.565, respectively]. Siemens programs, SHELXTL PLUS (release 4.21/V), were used for phase determination and structure refinement, and atomic coordinates and isotropic and anisotropic temperature factors for all non-hydrogen atoms were refined by means of blocked full-matrix least-squares procedures. The refinement converged at R = 6.85% and R_w = 8.67%. The background in the electron density map was 0.64 e/Å^3.

(12) Potts, K. T.; Gheysen Raiford, K. A.; Keshavarz-K, M. *J. Am. Chem. Soc.* **1993**, *115*, 2793.
(13) (a) Potts, K. T.; Usifer, D. A.; Guadalupe, A. R; Abruña, H. D. *J. Am. Chem. Soc.* **1987**, *109*, 3961. (b) Potts, K. T.; M. J. Cipullo, M. J.; Ralli, P.; Theodoridis, G. *J. Org. Chem.* **1982**, *47*, 3027. (c) Cuenoud, B.; Schepartz, A. *Tetrahedron Lett.* **1991**, *32*, 3325; ref 3a.
(14) We thank Dr. R. Milberg, University of Illinois, for these data.

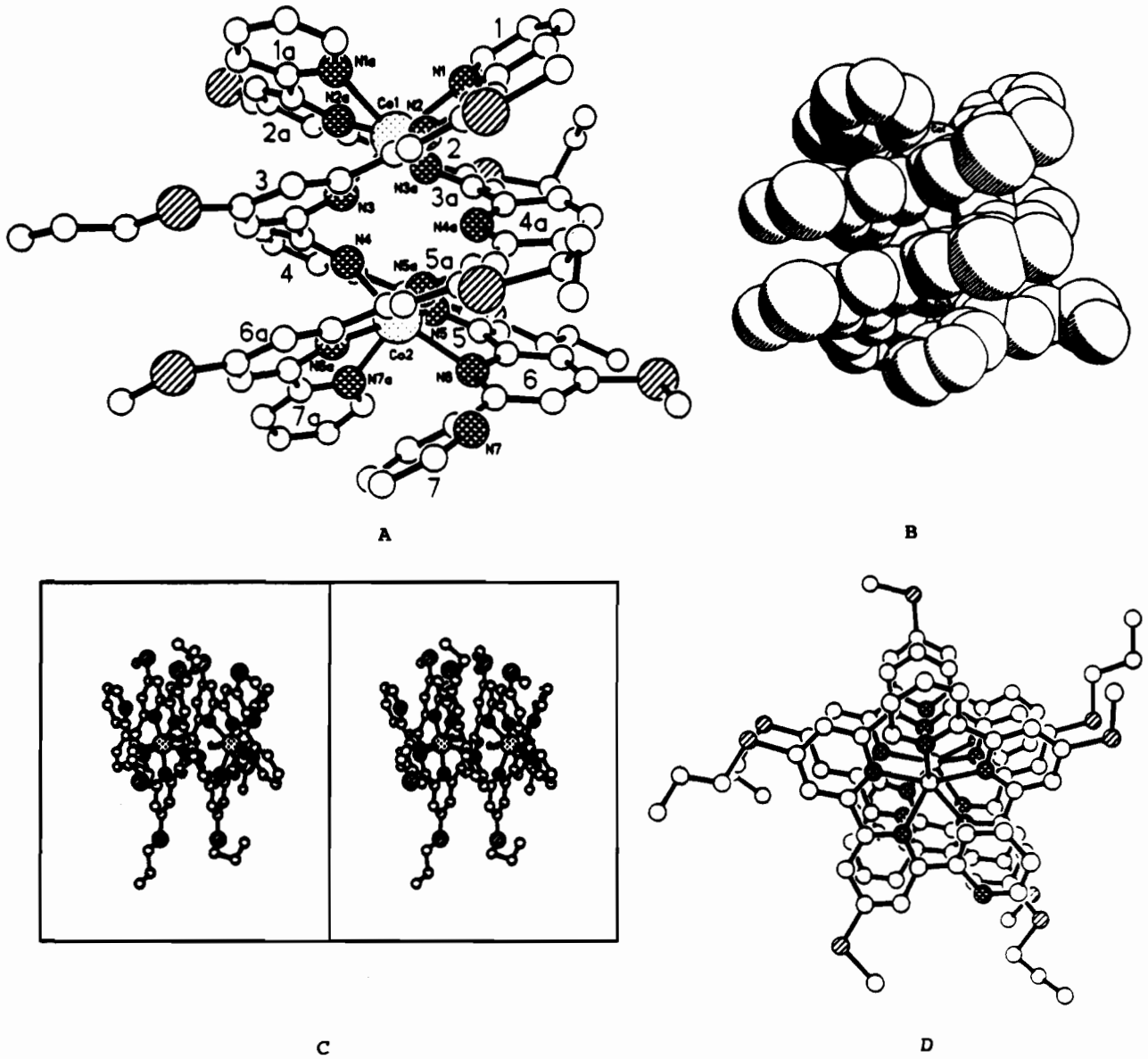

Figure 1. X-ray structure of complex **2**: A, view showing the right-handed (P) double-stranded helix; B, space-filling representation; C, stereotopic view; D, view skewed to the Co–Co axis showing the pronounced stacking in the complex.

Results and Discussion

(a) Co(II) Complexes. Reaction of the ligand **1** with $Co(OAc)_2 \cdot 4H_2O$ in methanol *(ambient temperature)* followed by counterion exchange with hexafluorophosphate resulted in a green salt (quantitative yield) whose analytical and FAB mass spectral data[14] [$M^+ - PF_6 = m/z$ 2116.7] established that it was a bimetallic complex $[Co^{II}(at\text{-}septipy)]_2^{4+}$ **(2)** (Scheme I). The X-ray structure of **2** is shown in Figure 1, and bond lengths and bond angles are reported in Table I. Figure 1 shows the double-stranded helical geometry of the assembly, which is the result of a series of twists about the C–C interannular bonds in each ligand strand. These strands behave as two terpy subunits and one uncoordinated pyridine ring, but the location of the uncoordinated pyridine ring in each strand is different: in one strand the middle pyridine ring (ring four) is uncoordinated and acts as an intersite bridge between two terpy subunits; in the other strand, a terminal pyridine ring is uncoordinated, and the remaining six pyridine groups behave as two terpy subunits similar to sexipyridine.[9] Thus, both the Co(II) centers have an octahedral N_6 environment. Interannular angles in each strand (Table I) show the deviation from coplanarity between the individual pyridine rings in each terpy subunit, and bond lengths(Table I)are comparable with those of bis(terpy)-cobalt(II) complexes.[15] The measured noncoordinated pyridine ring N–Co distance in strand 1 is 3.039 Å to Co(1) and 3.054 Å to Co(2). These distances preclude a heptacoordinated (N7) cobalt species.[3a] The helix in **2** has a pitch height of 10.92 Å, and the Co–Co distance is 4.606 Å. The π–π interaction between all pyridine rings in the assembly (Figure 1) produced five sets of stacks: four sets of triple stacks and a set of double stacks, with an average distance between the pyridine rings of 3.40 Å. Along with this π–π interaction an additional set of stacks involving the alkylthio sulfur atoms is clear from Figure 1. Three sets of two sulfur atoms have an average S–S distance of 3.871 Å, a distance slightly longer than the sum of the van der Waal radii (3.63 Å).

The electrochemical characterization of the at-septipyridine complexes of cobalt and copper was carried out by cyclic voltammetry in CH_3CN/0.1 M TBAP, and voltammetric data for the complexes are presented in Table II. The voltammetric response of the cobalt complex $[Co^{II}(at\text{-}septipy)_2]^{4+}$ **(2)** exhibited a single oxidation wave at +0.835 V, which we ascribe to a metal-localized process, as well as reductions at –0.635, –0.77, and –1.37 V (Figure 2). The peak current of the oxidative wave was about twice that of the reductions, suggesting that this is a two-electron process. In fact, constant potential electrolysis at an

(15) Figgis, B. N.; Kucharski, E. S.; White, A. H. *Aust. J. Chem.* **1983**, *36*, 1527, 1537.

Table I. Interannular Angles (deg) and Bond Lengths (Å) of Complex **2**

Interannular Angles in the First Strand

	1a	2a	3a	4a	5a	6a	7a
1a		23.7	33.8	49.6	36.8	26.7	23.7
2a			14.2	43.9	46.7	46.7	47.3
3a				32.7	43.7	50.6	55.6
4a					27.3	46.6	59.6
5a						21.0	35.9
6a							15.2

Interannular Angles in the Second Strand

	1	2	3	4	5	6	7
1		11.2	34.4	60.8	56.3	31.2	12.7
2			23.8	55.4	54.2	34.6	1.5
3				40.2	46.4	42.5	22.2
4					15.7	40.7	54.4
5						29.5	53.6
6							34.8

N–Co Bond Lengths (Å)

N(1a)–Co(1)	2.379(6)	N(1)–Co(1)	2.175(5)
N(2a)–Co(1)	2.081(5)	N(2)–Co(1)	2.028(4)
N(3a)–Co(1)	2.173(5)	N(3)–Co(1)	2.245(5)
N(5a)–Co(2)	2.186(4)	N(4)–Co(2)	2.293(5)
N(6a)–Co(2)	2.085(5)	N(5)–Co(2)	2.043(5)
N(7a)–Co(2)	2.291(5)	N(6)–Co(2)	2.256(5)

Nonbonded N–Co Distances

N(4a)–Co(1)	3.039(5)	N(7)–Co(2)	4.612(5)
N(4a)–Co(2)	3.054(5)		

Angles in the Distorted Octahedron of Co(1)

N(1)–Co–N(2)	76.0(2)	N(1)–Co–N(3)	151.4(2)
N(2)–Co–N(3)	75.6(2)	N(1)–Co–N(1a)	96.0(2)
N(2)–Co–N(1a)	81.7(2)	N(3)–Co–N(1a)	83.4(2)
N(1)–Co–N(2a)	112.8(2)	N(2)–Co–N(2a)	152.3(2)
N(3)–Co–N(2a)	94.2(2)	N(1a)–Co–N(2a)	71.5(2)
N(1)–Co–N(3a)	83.7(2)	N(2)–Co–N(3a)	132.3(2)
N(3)–Co–N(3a)	113.5(2)	N(1a)–Co–N(3a)	143.8(2)
N(2a)–Co–N(3a)	75.3(2)		

Angles in the Distorted Octahedron of Co(2)

N(4)–Co–N(6)	149.7(2)	N(4)–Co–N(5)	74.3(2)
N(4)–Co–N(5a)	113.2(2)	N(5)–Co–N(6)	75.4(2)
N(6)–Co–N(5a)	84.7(2)	N(5)–Co–N(5a)	129.9(2)
N(5)–Co–N(6a)	154.4(2)	N(4)–Co–N(6a)	93.3(2)
N(5a)–Co–N(6a)	75.5(2)	N(6)–Co–N(6a)	115.4(2)
N(5)–Co–N(7a)	84.4(2)	N(4)–Co–N(7a)	85.6(2)
N(5a)–Co–N(7a)	143.4(2)	N(6)–Co–N(7a)	94.0(2)
N(6a)–Co–N(7a)	72.1(2)		

applied potential of +1.10 V yielded an n value of 1.9 ± 0.1, consistent with this. The oxidation potential was significantly more positive than that of the complex[9,13a] $[Co^{II}(mt\text{-}terpy)_2][PF_6]_2$ (mt = methylthio) as well as of the complex $[Co^{II}(terpy)_2][PF_6]_2$ which are oxidized at +0.21 and +0.27 V, respectively. It is interesting that a single, two-electron wave was observed (as opposed to two, one-electron waves), since this is in contrast to the behavior of the closely related double-stranded helical $[Co^{II}(mt\text{-}sexipyridine)]_2^{4+}$ complex for which we observed[9] two, one-electron oxidations at potentials of +0.93 and +1.32 V, respectively. This last observation is consistent with significant metal–metal interactions in the dicobalt sexipyridine complex. The fact that in the septipyridine complex only one wave was observed strongly suggests that there is no interaction between metal centers.

Scheme I

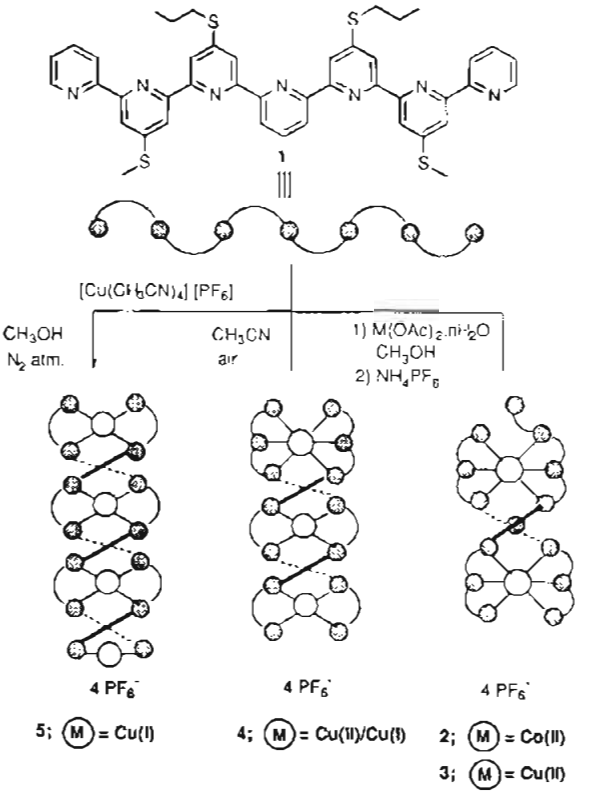

Such a difference in behavior is somewhat surprising and is likely due to differences in the structures of the two complexes, even though in both complexes the cobalt centers have octahedral (N_6) environments.

(b) Copper Complexes. The ligand **1** in the presence of copper ions at both oxidation states and under different reaction conditions resulted in a group of di-, tri-, and tetrametallic complexes (Scheme I). With $Cu^{II}OAc{\cdot}H_2O$ in methanol (*ambient temperature*) followed by counterion exchange with hexafluorophosphate, an olive-green salt was obtained which crystallized from CH_3NO_2/diethyl ether as green prisms. Analytical, FAB mass spectral data [$M^+ - PF_6 = m/z$ 2126.7], and electrochemical data established its $[Cu^{II}(at\text{-}septipy)]_2^{4+}$ composition, which, by analogy to **2**, was assigned as a double-stranded helical structure **3**. However, the position of the uncoordinated pyridine rings cannot be assigned. The N_6 octahedral environment around both copper ions is based on our earlier observation[9] of a double-stranded helicate obtained from Cu(II) (methylthio)sexipyridine, which was established by X-ray crystal analysis.

A colorless solution of the ligand **1** in oxygen-free methanol (*ambient temperature*, inert atmosphere) with an excess of $[(CH_3CN)_4Cu^I][PF_6]$ gave a dark-brown complex (quantitative yield) whose analytical and FAB mass spectral data, together with electrochemical data (see below), established its $[Cu^I_4(at\text{-}septipy)_2]^{4+}$ tetrametallic nature. The band maxima (λ_{max}) and molar absorptivities (ϵ) due to π–π^* transitions in the UV region, as well as metal to ligand charge-transfer (MLCT) transitions in the visible region, a unique characteristic of Cu(I) oligopyridine

Table II. Formal Potentials vs SSCE for Co and Cu Complexes of at-septipyridine[a]

complex	$E^{\circ\prime}$ (V) [ΔE_p (mV)] (CH_3CN)	UV/vis: λ_{max} [ϵ ($cm\ M)^{-1}$] (CH_3CN)
$[Co^{II}(at\text{-}septipy)]_2^{4+}$ (**2**)	+0.835* [100], –0.635 [80], –0.77 [80], –1.37 [90]	198 [5.1 × 10^4], 220 [4.9 × 10^4], 249 [4.7 × 10^4], 434 [4.8 × 10^3], 574 [2.5 × 10^3]
$[Cu^I_4(at\text{-}septipy)_2]^{4+}$ (**5**)	+0.02 [80], +0.44 [80], +0.84 [80], +1.08 [80], –1.11 [60], –1.27 [70], –1.49 [irrev]	210 [7.1 × 10^4], 288 [4.9 × 10^4], 350 (sh), 422 [1.1 × 10^4], 576 [5.7 × 10^3]
$[Cu^{II}Cu^I_2(at\text{-}septipy)_2]^{4+}$ (**4**)	+0.01 [160], +0.43 [160], +0.82 [220], –1.42 [100], –1.62 [100], –1.83 [irrev]	202 [9.7 × 10^4], 232 [9.3 × 10^4], 294 [9.3 × 10^4], 410 [6.7 × 10^4], 570 [3.6 × 10^3]
$[Cu^{II}(at\text{-}septipy)]_2^{4+}$ (**3**)	+0.05 [130], +0.24 [190]	298 [1.3 × 10^5], 302 [1.4 × 10^5]

[a] Except where stated, all processes are one-electron transfer. An asterisk indicates a two-electron wave.

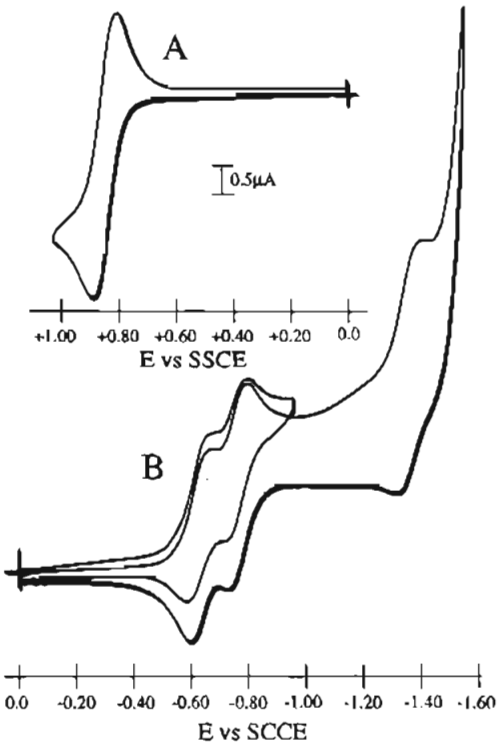

Figure 2. Cyclic voltammogram of $[Co^{II}(at\text{-}septipy)]_2^{4+}$ (**2**) in CH_3CN/0.1 M TBAP: A, oxidation; B, reduction.

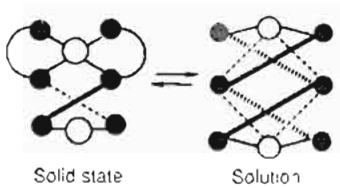

Figure 3. Solid-state and solution representation of the (terpyridine)-copper(I) complex.[4g]

complexes,[16] are listed in Table II. Structure **5** (Scheme I) represents one of the ways of accommodating four Cu(I) cations in three tetrahedral and one linear coordination environments. This representation is analogous to the solid-state structure found[4g] for the double-helical Cu(I) terpyridine complex, as well as that of Cu(I) quinquepyridine complexes.[9] However, the NMR spectra of these complexes show that they have highly symmetrical structures with D_2 symmetry in solution. This symmetry may be accommodated by the complexes assuming in solution a symmetrical diamond-type structure,[17] shown schematically for the (terpyridine)copper(I) complex in Figure 3, and this assignment was discussed in more detail previously.[4g]

The ^1H NMR spectra (Figures 4 and 5) of the ligand **1** and complex **5** are especially informative and provide an insight into the stability of the complex in solution, its solution structure, and its chiral nature. The NMR spectrum of the complex which was precipitated from the reaction mixture establishes that the self-assembly process results in one product only. The chemical shifts of the protons in the complex occurred appreciably upfield to those of the free ligand with a significant change in the overall pattern of the chemical shifts. Similar changes have been observed[4g,9] previously for the protons in Cu(I) double-stranded helical complexes derived from alkylthio-substituted oligopyridines. These observed upfield shifts are due to the helical nature of the complex in which the aromatic protons are positioned in the shielding zone of the neighboring aromatic rings. These changes in chemical shifts are in contrast to those observed for

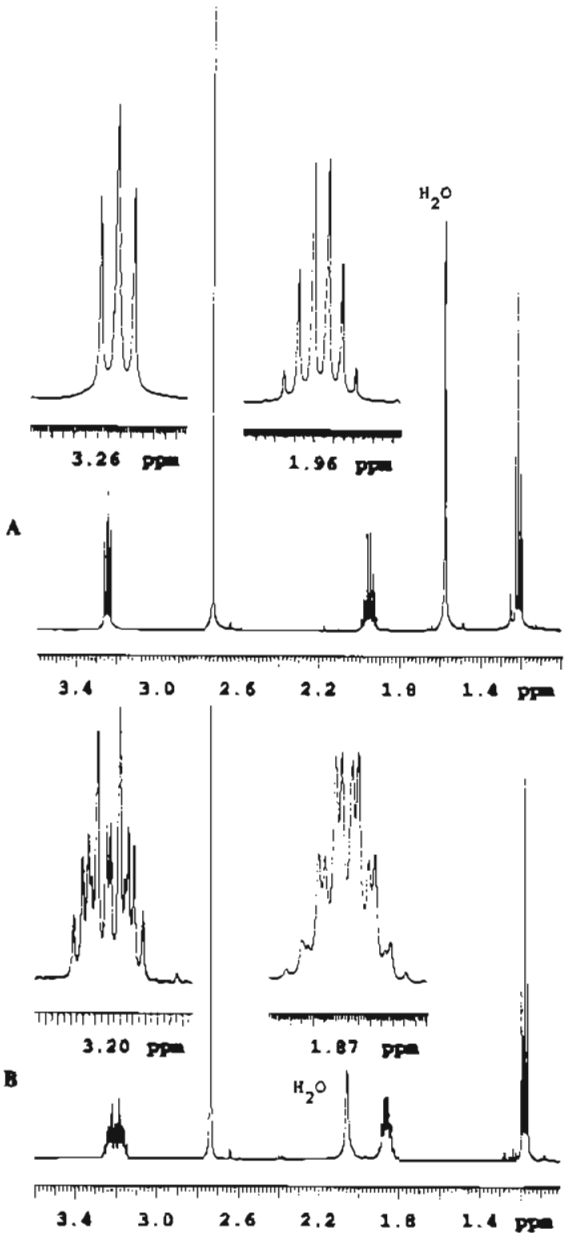

Figure 4. ^1H NMR spectra (500 MHz) of the aliphatic region of (A) the ligand **1** in $CDCl_3$ and (B) the complex **2** in CD_3NO_2. Insets are the expanded multiplets of the $S\text{–}CH_2CH_2$ protons.

the corresponding protons in the simple tetrahedral (bipyridine)-copper(I) complex[18] $[L_2M]^+$ in which the overall trend is a downfield shift except for H_3. This proton's upfield shift is due to a ligand conformational change from transoid to cisoid upon complexation with Cu(I) ions.

Symmetry elements in the ligand **1** reduce the observable number of aromatic protons to 10 (out of a total of 19 aromatic protons). The same number of aromatic protons were observed in the complex **5**, where there are a total of 38 aromatic protons in both strands. The number of aromatic protons suggests that, in solution, the complex **5** has the same type of C_2 symmetry axis presents which bisects pyridine ring four. Thus the trend observed for Cu(I) terpyridine and Cu(I) quinquepyridine complexes to adopt more symmetrical structures in solution is followed in the Cu(I) septipyridine complex. The representation used in Scheme I for complex **5** should be considered to be representative only of one of the possible solid-state structures.

This high degree of symmetry is also consistent with the observation of only one type of *S*-*n*-propyl group (out of four)

(16) Day, P.; Sanders, N. J. *J. Chem. Soc. A* **1967**, 1530. For recent references to this topic, see: Pfeil, A.; Lehn, J.-M. *J. Chem. Soc., Chem. Commun.* **1992**, 838.

(17) Alemany, P.; Alvarez, S. *Inorg. Chem.* **1992**, *31*, 4265.

(18) Dietrich-Buchecker, C. O.; Marnot, P. A.; Sauvage, J.-P. *Nouv. J. Chim.* **1984**, *8*, 573.

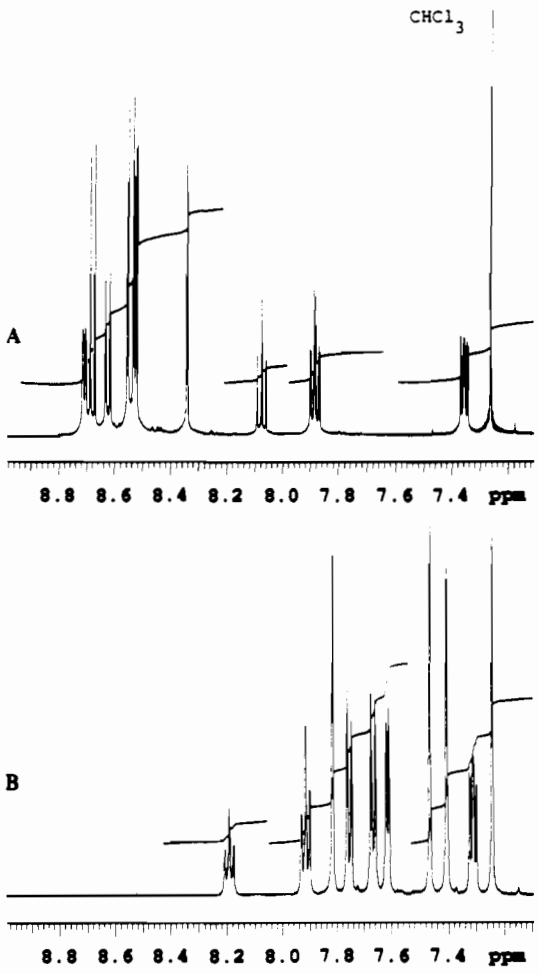

Figure 5. ^{1}H NMR spectrum (500 MHz) of the aromatic region of (A) the ligand **1** in $CDCl_3$ and (B) the complex **2** in CD_3NO_2.

and one type of SCH_3 group (out of four). As was observed in earlier work,[4g,9] the SCH_2R ($R \neq H$) group acts as an NMR probe for determining the helical chirality of a molecule. The enantiotopic S-CH_2- group in S-CH_2-CH_2-CH_3 has an A_2 spin system (triplet) in the achiral ligand **1**, whereas, when the -CH_2- group is situated in a chiral environment (the helix), it becomes diastereotopic and its spin system[19] changes to an AB type (multiplet). This effect on the second -CH_2- group is considerably depressed, and these changes in spin systems are shown in Figure 2.

Reaction of **1** with $[Cu^I(CH_3CN)_4][PF_6]$ in acetonitrile in the presence of air resulted in a black complex that was precipitated from the initial dark-brown reaction mixture with diethyl ether. It crystallized from CH_3NO_2/Et_2O as black prisms, and analytical, FAB mass spectral data, and the electrochemical data below established that the complex was the trimetallic species $[Cu^{II}/Cu^I_2(at\text{-}septipy)_2]^{4+}$ (**4**) (Scheme I). This requires a mixed-valence system with two Cu(I) ions and a Cu(II) ion in tetrahedral and octahedral environments, respectively. The near-IR spectrum (Figure 6) showed a broad absorption centered at 1420 nm [ϵ = 79 (cm M)$^{-1}$], which is absent in both homovalence systems. This absorption, an intervalence electron-transfer (IT) transition between the mixed-valence copper centers is clear evidence[7] for electron-delocalization and metal–metal coupling between the copper centers in this complex. Air oxidation of the tetrametallic complex **5** also gives the complex **4**.

The electrochemical behavior of the copper complexes of at-septipyridine is closely related to that of the other odd-numbered (oligopyridine)copper complexes. In the case of $[Cu^I_4(at\text{-}septipy)_2]^{4+}$ (**5**), four reversible (note that in Figure 7 the potential sweep was reversed after each individual redox process and a ratio of peak currents of unity clearly established the chemically reversible nature of each of these processes at a sweep rate of 100 mV/s), one-electron oxidations were observed at potentials of +0.02, +0.44, +0.84, and +1.08 V (Figure 7), respectively. The peak currents for all four waves were virtually identical, as would be anticipated. In addition, rotating-disk electrode voltammetry as well as the measurement of the rest potential, established that all four processes are oxidations, consistent with our assignment of four Cu(I) units in the complex.

Similarly, the complex $[Cu^{II}/Cu^I_2(at\text{-}septipy)_2]^{4+}$(**4**) exhibited three, well-resolved reversible redox processes (Figure 8) at potentials of +0.01, +0.43, and +0.82 V, respectively. Again, rotating-disk electrode voltammetry (Figure 9) as well as a measurement of the rest potential were also consistent with the oxidation-state assignments as being one Cu(II) and two Cu(I) ions; that is, there were two anodic [Cu(I) → Cu(II)] and one cathodic [Cu(II) → Cu(I)] waves. Finally, the $[Cu^{II}(at\text{-}septipy)]_2^{4+}$ complex exhibited two, one-electron redox processes with formal potentials of +0.05 and +0.24 V, respectively. In rotated disk electrode experiments, these appeared as two cathodic waves, establishing that they corresponded to reductions which we ascribe to Cu(II) → Cu(I) processes.

As we and others[4] have found earlier for copper complexes of related oligopyridines, these copper (at)-septipyridine helicates also undergo interesting redox-state induced transformations. These changes were followed spectroelectrochemically where changes in the visible spectrum were monitored as a function of applied potential (Figures 10 and 11). Figure 10 presents spectra for acetonitrile solutions of complexes **3**–**6**. We employed these spectra as guidelines for identifying intermediate species in spectroelectrochemical measurements. Figure 11 presents a series of spectra (taken at 3-min intervals) for a solution of **5** as the

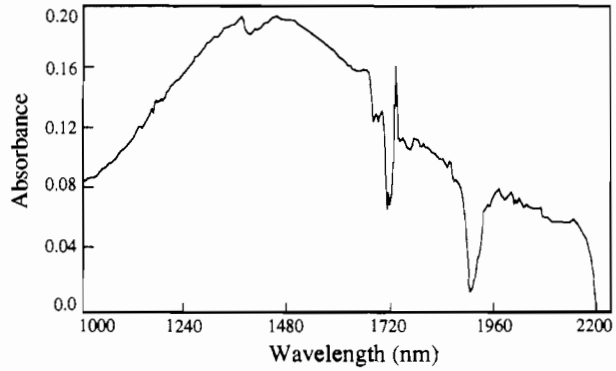

Figure 6. Intervalence electron-transfer transition for complex **4**.

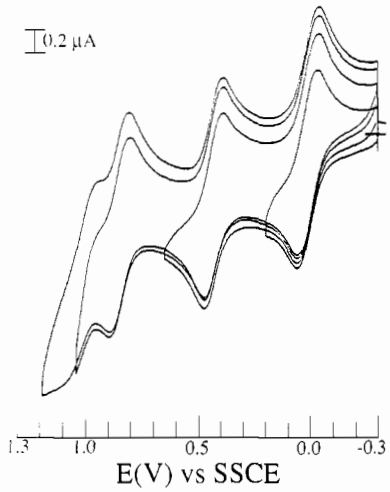

Figure 7. Cyclic voltammogram of $[Cu^I_4(at\text{-}septipy)]_2^{4+}$ (**5**) in CD_3NO_2/0.1 M TBAP.

(19) For a general discussion, see: Jennings, W. B. *Chem. Rev.* **1975**, *75*, 307. For similar observations, see refs 4c and 5.

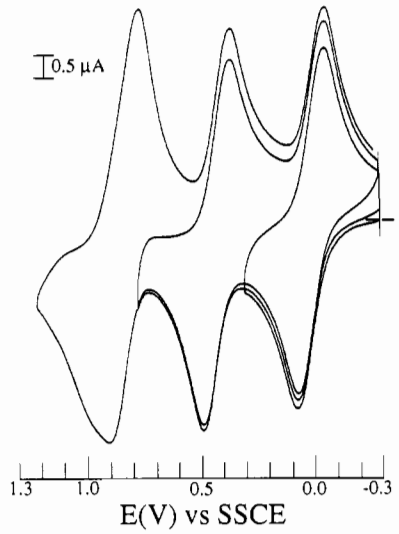

Figure 8. Cyclic voltammogram of $[Cu^{II}/Cu^{I}_2(at\text{-}septipy)_2]^{4+}$ (**4**) in CH_3CN/0.1 M TBAP.

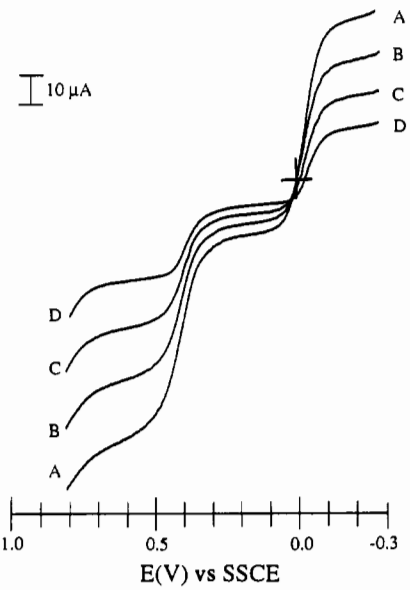

Figure 9. Rde voltammograms at (A) 900, (B) 500, (C) 250, and (D) 100 rpm for $[Cu^{II}/Cu^{I}_2(at\text{-}septipy)_2]^{4+}$ (**4**) in CD_3CN/0.1 M TBAP.

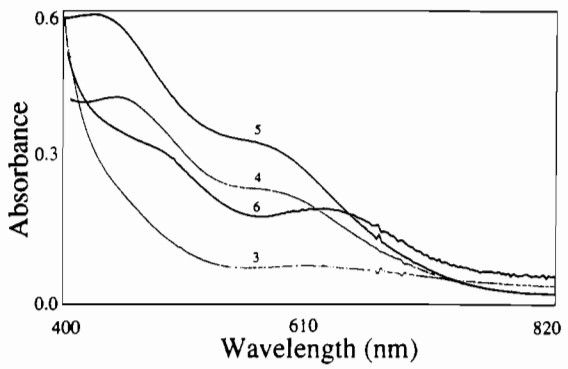

Figure 10. Visible spectra of complexes **3**–**6** in CH_3CN.

potential was systematically varied. Initially, the applied potential was –0.3 V. At this value no redox process would be anticipated and the spectrum (topmost trace a in Figure 11) is that of the complex where all copper ions are present as Cu(I). (Compare this spectrum with that presented in Figure 10 for **5**.) The applied potential was then changed to +0.20 V where oxidation takes place to yield complex **4**. As can be seen in Figure 11, the spectral changes observed are consistent with such a transformation (compare spectrum labeled b with that for **4** in Figure 10). Similarly, after adjustment of the potential to +0.6 and +0.9 V,

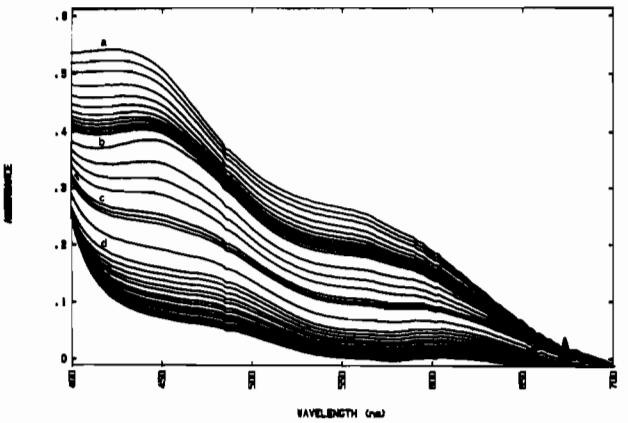

Figure 11. Changes in the visible spectrum of complex **5** on oxidation at a controlled potential. Spectra labeled a, b, c, and d correspond to applied potentials of –0.30, +0.20, +0.60, and +0.90 V, respectively.

Scheme II

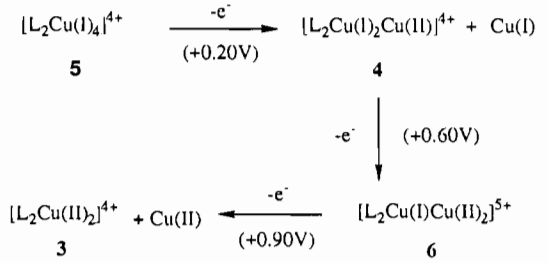

complexes **6** and **3**, respectively, were generated. Again, the species observed at the above mentioned potentials (see spectra c and d in Figure 11) were very similar to those of known samples of complexes **6** and **3** as shown in Figure 10.

There are some additional observations that can be made. First of all, these transformations are relatively slow. This could have been ascertained from the cyclic voltammogram in Figure 7, which showed that at 100 mV/s all redox processes were chemically reversible. The slowness of these transformations could well be due to a large activation energy associated with the significant changes involved in these transformations. However, the fact that the spectral changes take place (albeit at a relatively slow rate; recall that in Figure 11 spectra were recorded every 3 min) and that the spectra of intermediate species compare very well with those of known compounds adds strong support to our analysis. In addition, the fact that isosbestic points were typically not observed would imply that we have multiple species present and not a simple equilibrium between two species. These redox-induced transformations are summarized in Scheme II.

Conclusions. Septipyridine, a new and versatile ligand, offers a variety of coordination geometries in double-stranded helical assemblies. The nature of the complex formed with the septipyridine ligand depends on the stereochemical preferences (or requirements) of the metal ion. With Co(II) and Cu(II), which favor octahedral coordination, the double-helical structure was formed with each ligand strand acting as two terpyridine subunits and each strand having one uncoordinated pyridine ring. Extensive stacking was evident in the Co(II) complex which probably favored, to some degree, the final coordination geometry of the complex and contributed to its stability in solution. With Cu(I), septipyridine follows the trend observed with the odd-numbered oligopyridines previously studied. A tetrametallic complex was formed, whose structure could be accommodated by a mixture of tetrahedral–linear coordination geometries in the solid state. In solution, the complex had a more symmetrical (D_2) geometry, most likely involving diamond-type structures. This tetrametallic complex had good stability in solution, as evidenced by the high degree of resolution of the diastereotopic protons in the *S*-*n*-propyl groups attached to two 4-pyridyl positions in the ligand. The solution stability of the tetrametallic complex is in sharp

contrast to that shown by (terpyridine)copper(I) complexes, which undergo facile oxidation in solution to the corresponding Cu(II) complexes unless special precautions are taken to modify terpyridine so that the resultant complex is sheltered from the environment.[48] The next odd-numbered oligopyridine, quinquepyridine, formed Cu(I) complexes whose stability in solution was enhanced relative to terpyridine complexes but they were less stable than the septipyridine complexes described here. Continuation of this trend would suggest that the copper complexes derived from novipyridine should be even more stable and this may give rise to a diverse group of products; these are currently being studied together with the coordination chemistry of other transition metals.

Septipyridine also gave a unique trimetallic mixed-valence complex which showed an intervalence transfer transition band in its near-infrared spectrum. The quantitative redox-induced transformations of the copper complexes which were followed spectroelectrochemically are of particular interest in electrochemical applications and recognition based on electronic configurations and are being studied in more detail.

Acknowledgment. We thank Dr. R. Kullnig for his interest and encouragement during the X-ray structural determination, the NSF (Grant CHE-9105906) and USPHS (Grant S-10RR06245) for funds for the purchase of the 500-MHz spectrometer, and American Cyanamid Co. and the Materials Science Center at Cornell University for support of this work.

Supplementary Material Available: Tables of structure determination parameters, atomic coordinates, bond distances, bond angles, anisotropic thermal parameters and hydrogen atom positions for complex **2** (16 pages). Ordering information is given on any current masthead page.